

## Zero lattice sound

Simon Hands<sup>1</sup> and Costas G. Strouthos<sup>2,3</sup>

<sup>1</sup>*Department of Physics, University of Wales Swansea, Singleton Park, Swansea SA2 8PP, United Kingdom*

<sup>2</sup>*Department of Physics, Duke University, Durham, North Carolina 27708, USA*

<sup>3</sup>*Division of Science and Engineering, Frederick Institute of Technology, Nicosia 1303, Cyprus*

(Received 14 June 2004; published 20 September 2004)

We study the  $N_f$ -flavor Gross-Neveu model in  $2 + 1$  dimensions with a baryon chemical potential  $\mu$ , using both analytical and numerical methods. In particular, we study the self-consistent Boltzmann equation in the Fermi liquid framework using the quasiparticle interaction calculated to  $O(1/N_f)$ , and find solutions for zero sound propagation for almost all  $\mu > \mu_c$ , the critical chemical potential for chiral symmetry restoration. Next we present results of a numerical lattice simulation, examining temporal correlation functions of mesons defined using a point-split interpolating operator, and finding evidence for phononlike behavior characterized by a linear dispersion relation in the long wavelength limit. We argue that our results provide the first evidence for a collective excitation in a lattice simulation.

DOI: 10.1103/PhysRevD.70.056006

PACS numbers: 21.65.+f, 11.10.Kk, 11.15.Ha, 67.80.Cx

### I. INTRODUCTION

Such is the perceived difficulty of performing non-perturbative lattice simulations of systems with nonzero baryon chemical potential  $\mu$  that it is often overlooked that, in those cases where simulations are possible, the information extracted considerably exceeds that coming from better understood simulations at nonzero temperature  $T$ . The reason is that for  $\mu/T \gg 1$  there is no stringent limitation on the number of temporal lattice spacings  $L_t$ , so that correlation functions in Euclidean time can be studied with good resolution. These functions encode all information about the spectrum of the system under study, including energies and widths of all quasiparticle and collective excitations. For instance, Two Color QCD spectral studies have revealed a scalar isoscalar Goldstone boson signalling the superfluid nature of the high density state [1], and evidence for an in-medium decrease in mass of the  $\rho$  meson [2]. In the Nambu–Jona-Lasinio model in  $2 + 1d$ , the quasiparticle dispersion relation  $E(k)$  is smooth for  $k \simeq k_F$  implying a well-defined Fermi surface, but anomalously slow temporal decay in the scalar isoscalar diquark channel signals a critical state characteristic of a thin film superfluid [3,4]. In NJL<sub>3+1</sub> by contrast, the scalar isoscalar diquark channel has a Goldstone pole, and the quasiparticle dispersion is gapped, providing evidence for superfluidity via orthodox BCS diquark pair condensation [5].

In Ref. [6], we have studied a still simpler model, the  $2 + 1d$  Gross-Neveu (GN) model describing  $N_f$  flavors of self-interacting fermions, with continuum Lagrangian

$$\mathcal{L} = \bar{\psi}(\not{\partial} + \mu\gamma_0)\psi - \frac{g^2}{2N_f}(\bar{\psi}\psi)^2. \quad (1)$$

As  $\mu$  is increased, the model exhibits a sharp first-order transition at a critical  $\mu_c$  from a phase where a fermion mass  $\Sigma_0$  is dynamically generated but baryon density

$n_B = \langle \bar{\psi}\gamma_0\psi \rangle$  vanishes to one where  $\Sigma_0 = 0$  and  $n_B \propto \mu^2$  [7]. By examining various temporal correlation functions, we were able to demonstrate many features of this high density phase. For example, the quasiparticle dispersion relation is again consistent with a sharp Fermi surface, a feature reinforced by the oscillatory behavior of meson wave functions as the spatial separation between quark and antiquark fields is increased, reminiscent of a phenomenon in many-body physics known as Friedel oscillation. Second, we studied the correlator of the scalar meson  $\sigma$  and found that, in contrast to its behavior in vacuum, in the high density phase it decays with a pole mass  $M_\sigma \simeq 2\sqrt{\mu(\mu - \mu_c)}$ , the value predicted to leading nontrivial order in  $1/N_f$ . Finally, we studied meson correlators at nonzero momentum with several different quantum numbers, and found that in general they decay algebraically rather than exponentially with Euclidean time, since it is usually possible to excite a particle-hole pair at the Fermi surface with zero energy cost.

There is a phenomenological model of interacting degenerate systems, originally due to Landau [8], known as the Fermi liquid. From a particle physics perspective it is conceptually simple; the dominant low energy excitations, the so-called quasiparticles, carry the same quantum numbers (spin, isospin, baryon number, ...) as free particles and holes, and can be viewed simply as dressed versions of the elementary quanta. Beyond the explicit breaking of Lorentz symmetry introduced by  $\mu \neq 0 \Rightarrow n_B \neq 0$ , there is no broken symmetry or order parameter which distinguishes the Fermi liquid from noninteracting degenerate fermions. However, if certain conditions are fulfilled, such as an effective interaction between quasiparticles which is both short-ranged and repulsive, then there is a massless bosonic excitation in the spectrum as  $T \rightarrow 0$ . Carrying zero baryon charge, it is a *phonon*, i.e., a quantum of a collective excitation called *zero sound* [9]. Sound propagation occurs in any elastic medium; zero

sound happens when the elasticity originates not from collisions between individual particles, but from the force on a single particle due to its coherent interaction with all others present in the medium. It can be pictured as a propagating distortion in the local shape of the Fermi surface, whose speed exceeds that of conventional “first” sound.

In [6], we found one meson channel whose temporal decay resembled that of an isolated pole rather than that of a particle-hole continuum, and which moreover yielded a phononlike dispersion relation  $\omega \propto k$ . In the current paper, we seek to build on our tentative identification of this state with zero sound, first by finding an analytic solution appropriate for  $\text{GN}_{2+1}$ , and second by performing a more refined numerical analysis in the channel of interest. In Sec. II we review the derivation of the self-consistent equation for zero sound propagation in the framework of orthodox Fermi liquid theory, and in Sec. III we solve this equation for the particular case of  $\text{GN}_{2+1}$ , using the  $O(1/N_f)$  expression for quasiparticle interactions derived in [6]. We find solutions for sound propagation for almost all  $\mu > \mu_c$ , with speed  $\beta_0 > \beta_F$ , the Fermi velocity, which is the characteristic scale for a degenerate system. In Sec. IV we present results of a numerical simulation of  $\text{GN}_{2+1}$ ; we apply orthodox meson spectroscopy techniques and find evidence for a state with dispersion  $\omega(k) \propto k$  in the small- $k$  limit. The propagation speed is of the same order as, but slightly less than, the Fermi velocity. Our results are summarized with a discussion about possible sources for the discrepancy in Sec. V.

## II. THEORETICAL BACKGROUND

We begin with a brief introduction of the theory behind sound propagation in degenerate systems, leaning heavily on the treatment in [10]. Consider a system of (quasi)particles with phase space distribution  $n$  given by

$$n(\vec{k}, \vec{x}, t) = n_0(\vec{k}) + \delta n(\vec{k}, \vec{x}, t) \quad (2)$$

and energy

$$\varepsilon(\vec{k}, \vec{r}, t) = \varepsilon_0(\vec{k}) + \delta \varepsilon(\vec{k}, \vec{r}, t), \quad (3)$$

where for states near the Fermi surface the equilibrium conditions are given by

$$\begin{aligned} n_0(\vec{k}) &= \{\exp[\varepsilon_0(\vec{k}) - \mu]/T + 1\}^{-1} \\ \varepsilon_0(\vec{k}) &\simeq \mu + \beta_F(|\vec{k}| - k_F). \end{aligned} \quad (4)$$

The parameters are Fermi momentum  $k_F$ , and Fermi velocity  $\beta_F \equiv |\vec{\nabla}_k \varepsilon_0(|\vec{k}| = k_F)|$ , which in general differ from their free field theory values. Small departures from equilibrium are described by

$$\delta \varepsilon(\vec{k}, \vec{x}, t) = \text{tr} \int \frac{d^d k'}{(2\pi)^d} \mathcal{F}(\vec{k}, \vec{k}') \delta n(\vec{k}', \vec{x}, t), \quad (5)$$

where  $d$  is the number of spatial dimensions and the trace is over internal degrees of freedom such as spin and flavor. The Fermi liquid interaction  $\mathcal{F}$  encodes the response of a single quasiparticle state to a change in the many-body distribution, and is thus nonzero only for interacting systems [8]. To leading order in any small expansion parameter,  $\mathcal{F}$  is equivalent to the matrix element for forward scattering [11]. A review of the Fermi liquid picture applied to relativistic systems is given in [12].

Departures from equilibrium are described by a transport (Boltzmann) equation

$$\frac{dn}{dt} = \frac{\partial \delta n}{\partial t} + \vec{\nabla} \delta n \cdot \vec{\nabla}_k \varepsilon_0 - \vec{\nabla}_k n_0 \cdot \vec{\nabla} \delta \varepsilon = I(n), \quad (6)$$

where we have used Hamilton's equations

$$\frac{\partial \vec{x}}{\partial t} = \vec{\nabla}_k \varepsilon; \quad \frac{\partial \vec{k}}{\partial t} = -\vec{\nabla} \varepsilon, \quad (7)$$

and dropped terms of  $O(\delta^2)$ . The term  $I(n)$  on the right-hand side is the collision integral describing the net number of scattering events into the phase space element  $d^d x d^d k$  per unit time. For oscillation frequency  $\omega$  with mean free time  $\tau$  between quasiparticle collisions, the dimensionless parameter  $\omega\tau$  governs which kind of excitation dominates. For  $\omega\tau \ll 1$ , collisions reestablish local thermodynamic equilibrium in each volume element, and ordinary *first sound* waves propagate with velocity  $\beta_1 = \sqrt{\partial p / \partial \varepsilon} \simeq k_F / \sqrt{d} \mu$ . For  $\omega\tau \gg 1$ , collisions are unimportant, and local thermodynamic equilibrium no longer holds. Since for a Fermi liquid  $\tau \propto T^{-2}$ , this situation holds near temperature zero, and the consequent excitations are known as *zero sound*.

With  $T = I = 0$ , we have

$$\begin{aligned} \vec{\nabla}_k \varepsilon_0 &= \beta_F \hat{m}; \\ \vec{\nabla}_k n_0 &= -\hat{m} \beta_F \delta(\varepsilon - \mu) = -\hat{m} \delta(|\vec{k}| - k_F), \end{aligned} \quad (8)$$

where  $\hat{m} \cdot \vec{k} = |\vec{k}|$ ,  $\hat{m} \cdot \hat{m} = 1$ . Specializing to oscillatory excitations at the Fermi surface of the form  $\delta n = \delta(\varepsilon - \mu) \Phi(\hat{m}) e^{i(\vec{k} \cdot \vec{x} - \omega t)}$ , we find the self-consistent zero sound equation [9]

$$\begin{aligned} (\omega - \beta_F \hat{m} \cdot \vec{k}) \Phi(\hat{m}) &= \hat{m} \\ &\cdot \vec{k} S_d k_F^{d-1} \text{tr} \oint d\Omega \mathcal{F}(\hat{m}, \hat{m}') \Phi(\hat{m}'), \end{aligned} \quad (9)$$

where the integral over the unit sphere is normalized to  $\oint d\Omega = 1$ , and the geometrical factor  $S_d \equiv 2/(4\pi)^{d/2} \Gamma(\frac{d}{2})$ .

## III. ANALYTIC SOLUTION

For the  $\text{GN}_{2+1}$  model considered here, the Fermi surface is a circle, and the Fermi liquid interaction a simple

function of the angle  $\theta$  between quasiparticle momenta. Quasiparticle interactions in the GN model are mediated by a scalar boson  $\sigma$ : To leading order in  $1/N_f$  in the chiral limit the interaction arises from the exchange contribution to forward scattering, is repulsive, and has been determined to be [6]

$$\mathcal{F}(\theta) = \frac{\pi}{4N_f(\mu - \mu_c)}(1 - \cos\theta), \quad (10)$$

where  $\mu_c$  is the critical chemical potential at which the transition from chirally broken vacuum to chirally symmetric quark matter takes place at  $T = 0$ . To leading order in  $1/N_f$   $\mu_c = \Sigma_0$ , the dynamically generated quark mass at  $T = \mu = 0$ . For reasons to be made clear below, we will generalize (10) to read  $\mathcal{F} \propto R - \cos\theta$  with  $R > 1$ .<sup>1</sup> Using (10) in (9) we derive

$$(\zeta - \cos\theta)\Phi(\theta) = G \cos\theta \oint \frac{d\theta'}{2\pi} [R - \cos(\theta - \theta')]\Phi(\theta'). \quad (11)$$

The variable  $\zeta = s + i\gamma$  is the ratio of phase velocity  $\beta_0 \equiv \omega/|\vec{k}|$  to Fermi velocity  $\beta_F$ . The constant  $G$  parametrizing the strength of the Fermi liquid interaction will be specified below.

To find a solution we attempt an ansatz of the form

$$\Phi(\theta) = \sum_n \frac{b_n \cos^n \theta + c_n \sin \theta \cos^n \theta}{\zeta - \cos \theta}. \quad (12)$$

After substituting this into (11), the integrals over  $\theta'$  can be performed using

$$\begin{aligned} \oint \frac{d\theta}{2\pi} \frac{\cos n\theta}{\zeta - \cos \theta} &= -\frac{2a^n}{a - a^{-1}}; \\ \oint \frac{d\theta}{2\pi} \frac{\sin \theta \cos n\theta}{\zeta - \cos \theta} &= 0 \end{aligned} \quad (13)$$

where  $a, a^{-1}$  are the roots of  $z^2 - 2\zeta z + 1 = 0$  and we specify  $|a| \leq 1$ . Equating coefficients of  $\cos^n \theta$  it is straightforward to show that the only nontrivial coefficients in (12) are  $b_1$  and  $b_2$ ; we arrive at the coupled system

$$\begin{aligned} b_1 &= -\frac{RG}{a - a^{-1}}[2b_1 a + b_2(1 + a^2)], \\ b_2 &= \frac{G}{a - a^{-1}}\left[b_1(1 + a^2) + \frac{b_2}{2}(3a + a^3)\right] \end{aligned} \quad (14)$$

and immediately deduce

<sup>1</sup>In principle this could arise through a small bare quark mass  $m$ , whereupon the exchange term yields  $R = 1 + m^2/\mu^2$  [12]. Note, though, that for  $m \neq 0$  there is also an *attractive* contribution from the direct term, which moreover is no longer  $O(1/N_f)$ .

$$\frac{b_2}{b_1} = \frac{a^{-2} - 1 - 2GR}{GR(a + a^{-1})}. \quad (15)$$

Substituting this back into (14) determines a cubic equation for  $a^2$ :

$$(a^2 - 1)\{Ga^4 + a^2[2RG^2 + G(3 - 4R) - 2] + 2\} = 0. \quad (16)$$

Discarding the trivial solution  $a^2 = 1$ , we find a regular real solution with  $a < 1$  exists for  $R > 2/(2 - G)$  and is given by

$$a^2 = \frac{1}{G}\{1 + (2R - \frac{3}{2})G - G^2R - \sqrt{[1 + (2R - \frac{3}{2})G - G^2R]^2 - 2G}\}. \quad (17)$$

The corresponding sound speed is given by

$$s = \frac{1}{2}(a + a^{-1}) > 1. \quad (18)$$

Note that since  $s > 1$  the denominators of (12),(13) are never zero; there is no necessity to specify a pole prescription to evaluate the integral and  $\gamma = 0$ . Physically this means the wave is undamped. There are no solutions of the form (12) with complex  $a$  which describe dissipative solutions with  $s < 1$  and  $\gamma \neq 0$ .

We now return to the issue of why it is appropriate to consider  $R > 1$  for the GN model in the chiral limit. The expression (10) is derived from the relation  $\mathcal{F}(\theta) = -\mathcal{A}(\theta)$ , where  $\mathcal{A}$  is the forward scattering amplitude for physical quasiparticles on the Fermi surface, and is valid only in the large- $N_f$  limit. Beyond this leading order it is necessary to consider a more general amplitude  $\mathcal{M}(\theta, q)$  with momentum transfer  $q = (q_0, \vec{q})$ . For quasiparticle forward scattering at the Fermi surface  $\mathcal{A} = \lim_{|\vec{q}| \rightarrow 0} \lim_{q_0 \rightarrow 0} \mathcal{M}(q)$ , whereas for the Fermi liquid interaction  $\mathcal{F} = -\lim_{q_0 \rightarrow 0} \lim_{|\vec{q}| \rightarrow 0} \mathcal{M}(q)$  [8] (see also [13]). Taking the noncommutativity of the limits into account yields the relation

$$-\mathcal{A}(\theta) = \mathcal{F}(\theta) + \frac{g k_F}{2\pi\beta_F} \oint \frac{d\theta'}{2\pi} \mathcal{A}(\theta') \mathcal{F}(\theta - \theta'), \quad (19)$$

where  $g$  is the degeneracy of single particle states resulting from the trace in (9). Expanding  $\mathcal{A}(\theta) = -\sum_n P_n \cos n\theta$ ,  $\mathcal{F}(\theta) = \sum_n Q_n \cos n\theta$ , we readily derive the general relation

$$Q_n = \frac{P_n}{1 - \frac{g k_F}{4\pi\beta_F} P_n}. \quad (20)$$

For the GN model the only nonvanishing coefficients are  $n = 0, 1$ ; we recover (11) with

$$\begin{aligned}
G &= \frac{2\tilde{G}}{2 + \tilde{G}}; \\
\tilde{G} &= \frac{g k_F}{8N_f \beta_F(\mu - \mu_c)} = \frac{g\mu}{8N_f(\mu - \mu_c)} + O(N_f^{-2}); \quad (21) \\
R &= \frac{2 + \tilde{G}}{2 - \tilde{G}} > \frac{2}{2 - G}.
\end{aligned}$$

A zero sound solution with  $s > 1$  therefore exists for all  $\mu \gtrsim 16N_f\mu_c/(16N_f - g)$ .

In Fig. 1 we plot  $s(\mu)$  for the model defined by  $g = 2$ ,  $N_f = 4$ ,  $\mu_c a = 0.16$  corresponding to the simulation results to be presented in the next section. Note that chemical potential is expressed in cutoff units. The plot only shows those solutions with  $\mu a \gtrsim 0.18$  for which the physical sound speed  $\beta_0 = s\beta_F$  is definitely subluminal, using the relation  $\lim_{\mu \rightarrow \infty} \beta_F = 1 - g/32N_f = \frac{63}{64}$  (note, though, that for finite  $\mu$  this probably overestimates  $\beta_F$ ) [6]. The plot shows  $s$  to be a rapidly decreasing function of  $\mu$ , although the scale does not permit the observation that  $\lim_{\mu \rightarrow \infty} [s(\mu) - 1] \simeq 0.202 \times 10^{-5} > 0$ .

To illustrate the form of the solution, we plot  $\Phi(\theta)$  for various  $\mu$  in Fig. 2. The wave function has nodes at  $\theta = \pm \frac{\pi}{2}$ , and is highly peaked in the forward direction, once again due to the causality restriction that  $s \sim 1$  implying the denominator of (12) is very small as  $\theta \rightarrow 0$ . This would appear to be a general feature of weakly interacting relativistic systems: Indeed, Fig. 2 shows the peak sharpen as  $\mu$  increases and hence  $G(\mu)$  decreases, until a constant profile is reached as  $\mu \rightarrow \infty$ .

#### IV. NUMERICAL RESULTS

We have simulated lattice-regularized versions of the GN model in  $2 + 1d$  with both  $Z_2$  and  $SU(2) \otimes SU(2)$  global chiral symmetries. The underlying lattice action uses staggered fermions: Further details of the formulation and simulation algorithm are given in [3,7]. Most of our results are from the  $Z_2$  version, for which unless otherwise stated the simulation parameters are identical to those of our previous study [6], namely  $N_f = 4$  and  $a/g^2 = 0.75$ , corresponding to a physical fermion mass at  $\mu = 0$  of  $\Sigma_0 a \simeq 0.17$ . We have studied both  $32^2 \times 48$  lattices (the volume used exclusively in [6]) and  $48^3$ ; the increased momentum resolution offered by the latter has proven to be important. All results are taken in the chirally restored phase, i.e., with  $\mu > \mu_c \simeq 0.16a^{-1}$ . Measured values for the baryon density in lattice units  $a = 1$  are given in Table I, and are to be compared to the saturation value  $n_B(\mu \rightarrow \infty) = N_f/2$ .

By analyzing the decay of the appropriate correlation function with Euclidean time, we have calculated the dispersion relations  $E(k)$  for the spin- $\frac{1}{2}$  quasiparticle, which carries a baryon charge, and  $\omega(k)$  for various meson states of the form  $\bar{\psi}\Gamma\psi$  which are best thought of as excitations formed from a particle-hole pair. We have simulated  $L_s^2 \times 48$  systems with  $L_s = 32$  and  $48$ , with  $\mu$  ranging from  $0.2$  to  $0.6$ , and have measured  $E(k)$ ,  $\omega(k)$  for  $\vec{k} = (k, 0)$  with  $k = 0, 2\pi/L_s, \dots, \pi/2$ . Note that the staggered fermion action is only invariant under translations of two lattice spacings, which restricts the space of accessible momenta. Further details can be found in [6].

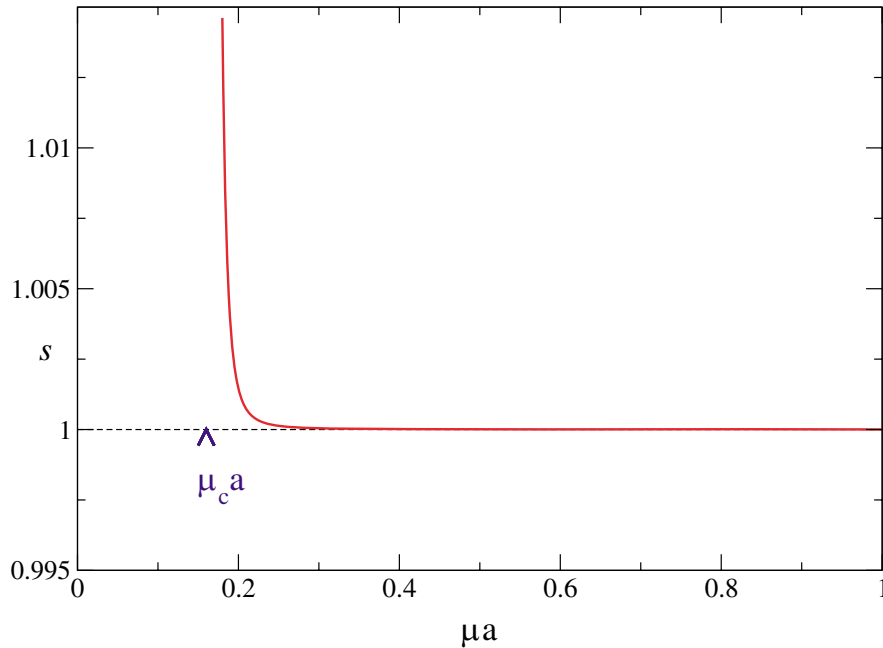


FIG. 1 (color online). The ratio  $s = \beta_0/\beta_F$  as a function of  $\mu a$  for the GN model with  $N_f = 4$ .

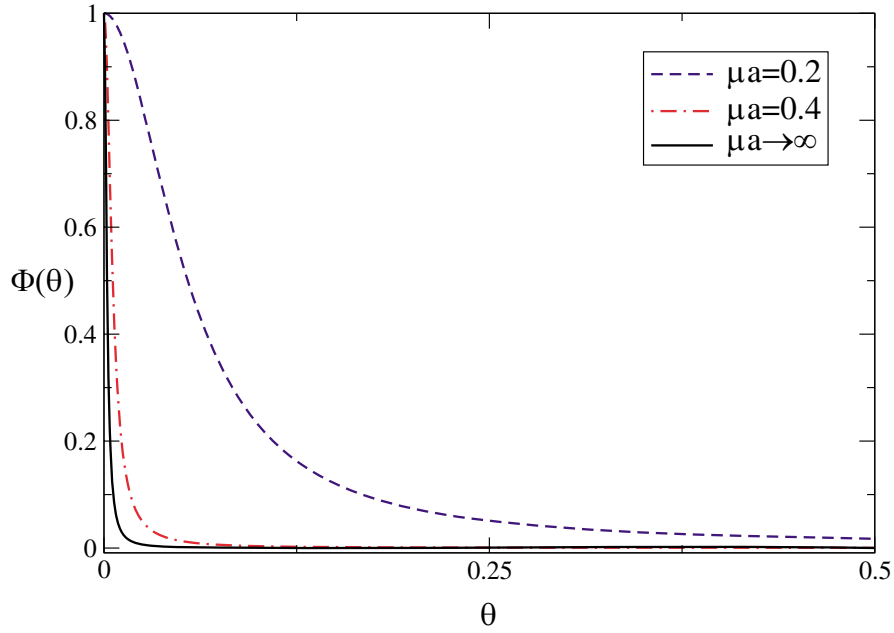


FIG. 2 (color online). Zero sound wave function  $\Phi(\theta)$  for representative values of  $\mu a$  for the GN model with  $N_f = 4$ .

The quasiparticle propagator  $\mathcal{G}(k, t)$  is measured using the formalism outlined in [4], although in this case an external diquark source term is not introduced, so the “anomalous” propagator of the form  $\langle \psi(0)\psi^{\dagger r}(x) \rangle$  vanishes. In the chirally restored phase  $\mathcal{G}(k, t)$  vanishes for  $t$  even; on the odd time slices we fit to the form

$$\mathcal{G}(k, t) = Ae^{-E_h(k)t} + Be^{-E_p(k)(L_t-t)}. \quad (22)$$

Note that due to the explicit breaking of time-reversal symmetry by  $\mu \neq 0$ , there is no requirement for  $A$  and  $B$  to be equal. On  $48^3$  acceptable fits were found for the most part for  $t \in [7, 43]$ , although the fitting window had to be reduced somewhat for  $\mu = 0.2, 0.3$ . Empirically we find that for small  $k$  the fit is dominated by a forward-propagating state (i.e.,  $A \gg B$ ) which is interpreted as a hole, and for large  $k$  by a backward-propagating state ( $A \ll B$ ) interpreted as a particle. The transition between particle and hole behavior is rather sudden, characteristic of a well-defined Fermi surface. In Fig. 3 we show  $E(k)$  with hole energies  $E_h$  plotted negative. Also shown are fits to the data with  $k > 0$  of the form

TABLE I. Baryon density  $n_B = \langle \bar{\psi}\gamma_0\psi \rangle$  for the  $Z_2$  model with  $g^{-2} = 0.75$ .

$\mu$	$n_B$
0.2	0.0226(2)
0.4	0.1040(2)
0.5	0.1730(2)
0.6	0.2788(2)
0.8	0.6254(2)

$$E(k) = -E_0 + D \sinh^{-1}(\sinh k), \quad (23)$$

i.e., that of a Fermi liquid with discretization effects taken into account, with effective Fermi momentum  $K_F$  and Fermi velocity  $B_F$  given by [4]

$$\begin{aligned} K_F &\equiv \sinh^{-1}(\sinh k_F) = \frac{E_0}{D}; \\ B_F &= \left. \frac{\partial \sinh(E + E_0)}{\partial \sinh k} \right|_{E=0} = D \frac{\cosh E_0}{\cosh K_F}, \end{aligned} \quad (24)$$

where  $E(k_F) = 0$ . The resulting  $K_F$ ,  $B_F$ , and  $K_F/\mu B_F$  are tabulated in Table II, and should be compared with the continuum values predicted in the large- $N_f$  approach for  $\mu \gg \mu_c$  [6]:

$$\begin{aligned} \beta_F &= 1 - \frac{g}{32N_f} \approx 0.984; \\ \frac{k_F}{\mu \beta_F} &= 1 - \frac{g}{16N_f} \approx 0.969. \end{aligned} \quad (25)$$

The agreement is at best qualitative; the computed  $O(1/N_f)$  corrections are so small that much better control over systematic effects would be required for a meaningful comparison with the data. For instance, the Fermi liquid parameters should be most accurately pinned down for  $\mu a \approx 0.7$  implying roughly equal numbers of points with  $k < k_F$  and  $k > k_F$ . Note also that analytic prediction of  $\beta_F$ ,  $k_F$  to  $O(1/N_f)$  for finite  $\mu$  strictly requires a knowledge of the gap equation to two loops, which is not yet available [6]. For the remaining analysis we will therefore assume the free field values  $K_F = \mu$ ,  $B_F = 1$ .

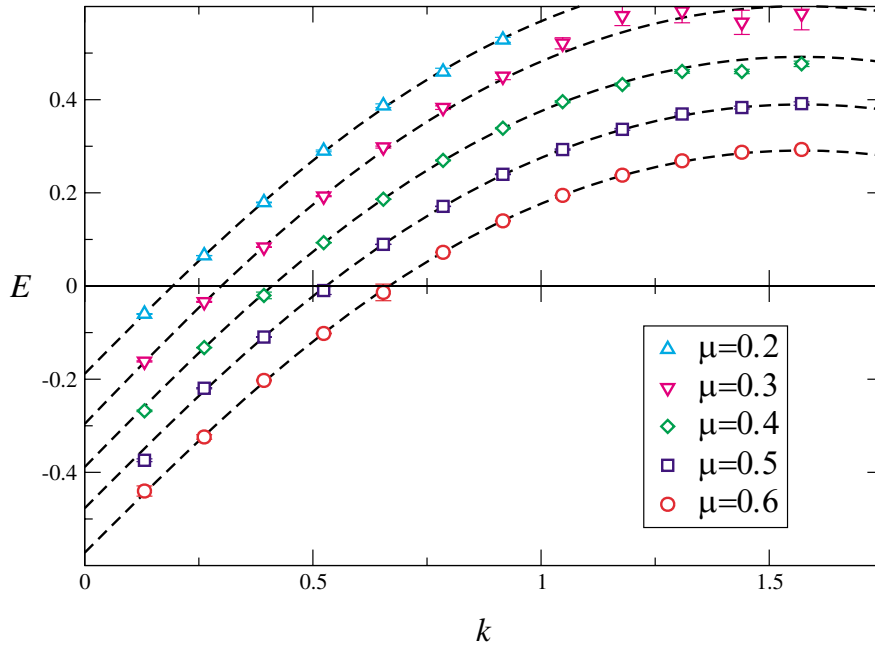


FIG. 3 (color online). Quasiparticle dispersion relation  $E(k)$  from simulations of the  $Z_2$  GN model on  $48^3$ .

We have observed a similar situation in simulations of the  $SU(2) \otimes SU(2)$  model on  $32^2 \times 48$  with coupling  $g^{-2} = 0.85$  chosen so that the vacuum fermion mass  $\Sigma_0$  matches that of the  $Z_2$  model at  $g^{-2} = 0.75$ . A much larger discrepancy in this model between the measured Fermi liquid parameters and the prediction (25) was reported in [4], probably due to the relatively small ratio  $(\mu - \mu_c)/\mu$  used in that study, implying that the Fermi liquid interaction is strong and higher order effects are important.

Next we consider the meson sector, i.e., correlators of the form

$$C_\Gamma(\vec{k}, t) \equiv \sum_{\vec{x}} \langle \bar{\psi} \Gamma \psi(\vec{0}, 0) \bar{\psi} \Gamma \psi(\vec{x}, t) \rangle e^{i\vec{k} \cdot \vec{x}}, \quad (26)$$

which carry zero baryon number. In Ref. [6] we showed that the generic large-distance behavior in any given channel is dominated by zero-energy particle-hole pairs, and as a result the decay is algebraic, i.e.,  $C_\Gamma(t) \propto t^{-\lambda(\vec{k})}$ , with the exponent  $\lambda$  determined by the geometry of the overlap between two Fermi disks with relative displace-

ment  $\vec{k}$  between their centers. A particularly favorable configuration occurs for  $|\vec{k}| \approx 2\mu$ , in which case the Fermi surfaces just kiss, and  $\lambda = \frac{3}{2}$ . In this paper we focus on point-split meson operators corresponding to spatial components of the conserved vector current, i.e., of the form

$$j_i(x) = \frac{\eta_i(x)}{2} [\bar{\chi}(x) \chi(x + \hat{i}) + \bar{\chi}(x + \hat{i}) \chi(x)], \quad (27)$$

where  $\chi, \bar{\chi}$  are staggered fermion fields,  $\eta_1(x) = (-1)^t$ , and  $\eta_2(x) = (-1)^{t+x_1}$ . Just as before we set  $\vec{k} = (k, 0)$ , and define  $C_\parallel$  in terms of the correlator  $\langle j_1(0) j_1(x) \rangle$  and  $C_\perp \sim \langle j_2(0) j_2(x) \rangle$ . In Fig. 4 we show  $|C_{\parallel,\perp}|(k, t)$  data taken on a  $48^3$  lattice at  $\mu = 0.5$ , for both  $k = \frac{\pi}{3} \approx 2\mu$  and  $k = \pi - \frac{\pi}{3}$  (the modulus is taken because we use a log-linear scale, and  $C$  fluctuates in sign). Whereas  $C_\perp$  and  $C_\parallel(k = \frac{\pi}{3})$  all show behavior consistent with algebraic decay (we are unable to extract a quantitative estimate for  $\lambda$  due to the difficulties of correcting for mirror-image sources on a finite system [14]), the decay in the  $C_\parallel(k = \pi - \frac{\pi}{3})$  channel is much faster, and resembles the exponential decay expected of an isolated pole. We have fitted it with the form

$$C_\parallel(\pi - k, t) = A \exp[-\Omega(k)t] + (-1)^t B \exp[-\omega(k)t], \quad (28)$$

in most cases employing data points with  $t \in [10, 38]$ .

For small  $k$ , the coefficient  $B \gg A$ , suggesting that the correlator is dominated by a pole in the alternating channel. In Fig. 5, we plot the resulting dispersion relation

TABLE II. Fermi liquid parameters resulting from fits of (23) to data from a  $48^3$  lattice (quoted errors are purely statistical).

$\mu$	$K_F$	$B_F$	$K_F/\mu B_F$
0.2	0.190(1)	0.989(1)	0.962(5)
0.3	0.291(1)	1.018(1)	0.952(4)
0.4	0.389(1)	0.999(1)	0.973(1)
0.5	0.485(1)	0.980(1)	0.990(2)
0.6	0.584(1)	0.973(1)	1.001(2)

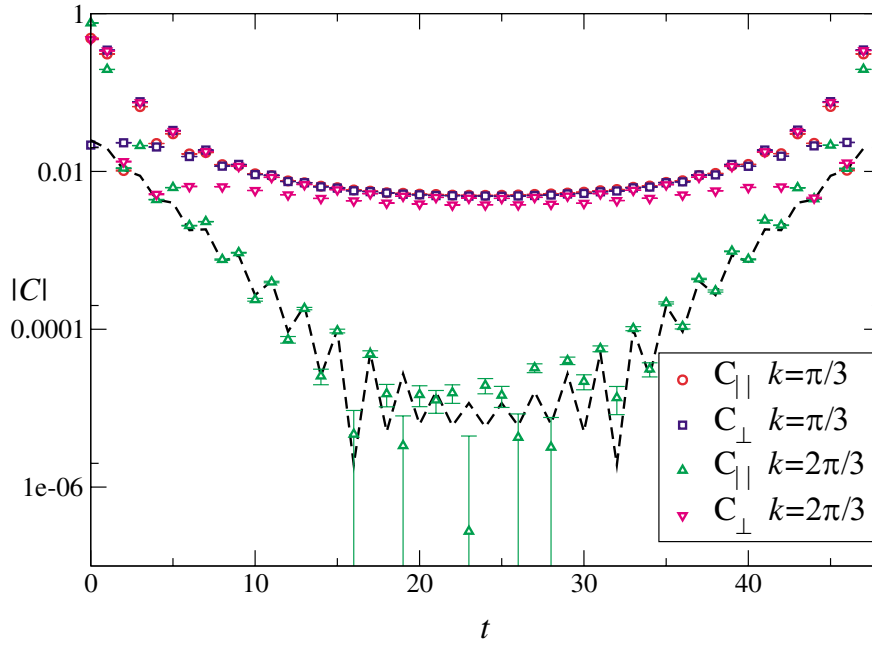


FIG. 4 (color online). Meson propagators  $|C_{\parallel}|$  and  $|C_{\perp}|$  for both  $k = \frac{\pi}{3}$  and  $\pi - \frac{\pi}{3}$  for  $\mu = 0.5$ . The dashed line shows a fit of the form (28).

$\omega(k)$  for  $\mu = 0.2, \dots, 0.6$ . The behavior  $\omega \propto k$  as  $k \rightarrow 0$  suggests the presence of a massless pole similar to that of a phonon. Support for this interpretation comes from recasting the meson bilinear in terms of continuumlike fields  $q^{\alpha a}$ ,  $\bar{q}^{\alpha a}$  having spinor index  $\alpha = 1, \dots, 4$  and “color” index  $a = 1, 2$  [15]. We obtain

$$(-1)^{x_1}(-1)^x \bar{\chi}(x) \eta_1 \chi(x + \hat{1}) \sim i \bar{q}(\gamma_0 \otimes \tau_2^*) q, \quad (29)$$

demonstrating that the excitation can be viewed as an oscillation of local baryon density.

Since we are attempting to simulate low temperatures  $T \ll \mu$ , our expectation is that the phonons are character

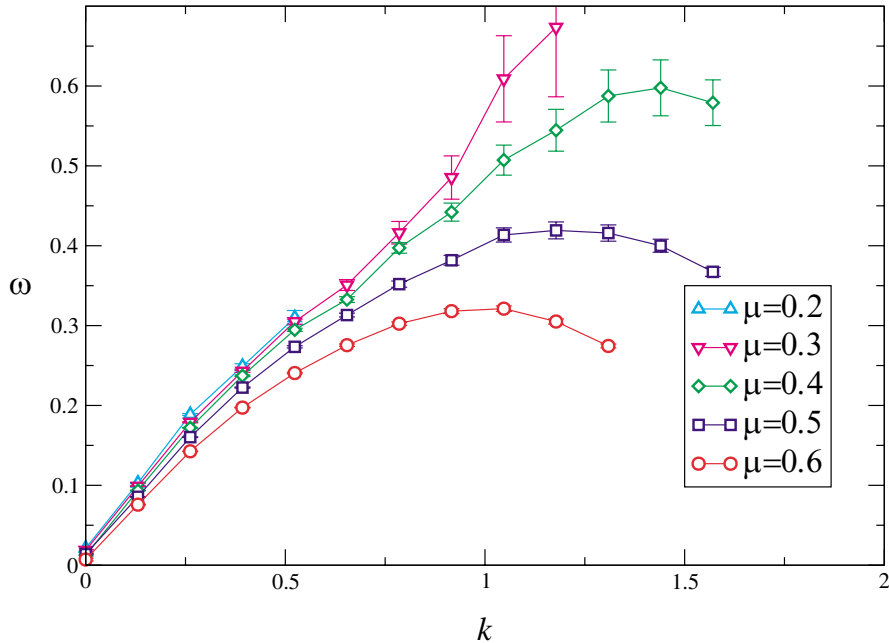


FIG. 5 (color online). Dispersion relation  $\omega(k)$  for various  $\mu$  for the channel defined by the correlator  $C_{\parallel}(\pi - k)$ . Data are from  $48^3$ .

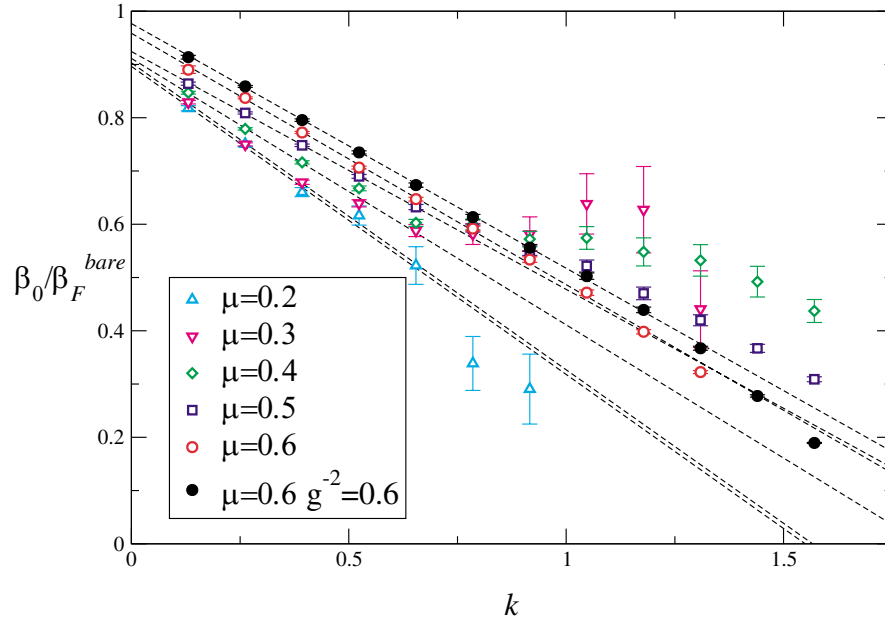


FIG. 6 (color online). Sound velocity  $\beta_0$  rescaled by the bare Fermi velocity  $\beta_F^{\text{bare}}$  for various  $\mu$ .

istic of zero sound and should be regarded as collective excitations of the degenerate ground state, rather than of first sound which relies on particle collisions to generate the elasticity of the medium, and which is therefore heavily damped for small  $T$  [10]. An obvious objection to this proposal is that the phase velocity  $\beta_0 = \omega/k$  derived from Fig. 5 has  $\beta_0 \sim 0.55\text{--}0.65$ , whereas the theoretical considerations of Sec. III imply that undamped oscillations in relativistic matter should have  $\beta_0 \approx 1$ . However, recall that although we are examining the  $k \rightarrow 0$  limit, we are trying to model a Fermi surface phenomenon on the lattice; the appropriate scale with which to compare  $\beta_0$  is the “bare” Fermi velocity (i.e., without the discretization correction modeled by (23) and

(24), which for free fields is given by

$$\beta_F^{\text{bare}} = \left. \frac{\partial E}{\partial k} \right|_{E=0} = \sqrt{\frac{1 - \sinh^2 \mu}{1 + \sinh^2 \mu}}. \quad (30)$$

In Fig. 6, we plot  $\beta_0/\beta_F^{\text{bare}}$  for  $k > 0$  using the  $48^3$  data of Fig. 5. There are two striking features. First, the ratio appears to extrapolate to a value rather closer to, though still smaller than, one as  $k \rightarrow 0$ , getting closer as  $\mu$  increases until for  $\mu = 0.6$  the intercept  $> 0.95$ . Second, for  $k \leq \frac{5\pi}{24}$  the curves are remarkably close to straight lines, implying a dispersion of the form  $\omega = sk - Fk^2$ . Figure 6 also shows fits of this form, and the resulting intercept and slope are given for all the systems studied in

TABLE III. Straight line fits to  $\omega/k\beta_F^{\text{bare}}$  vs  $k$  (quoted errors are purely statistical).

$\mu$	$48^3$		$32^2 \times 48$	
	$s$	$F$	$s$	$F$
$Z_2$ ( $g^{-2} = 0.75$ )				
0.2	0.896(8)	0.578(4)	...	...
0.3	0.903(5)	0.576(20)	...	...
0.4	0.911(4)	0.500(16)	0.894(5)	0.552(15)
0.5	0.924(3)	0.447(9)	0.961(3)	0.575(8)
0.6	0.959(2)	0.472(4)	0.950(2)	0.425(2)
0.7	...	...	1.033(3)	0.556(8)
$Z_2$ ( $g^{-2} = 0.6$ )				
0.6	0.977(2)	0.460(5)	...	...
$SU(2) \otimes SU(2)$ ( $g^{-2} = 0.85$ )				
0.5 $I_3 = 1$	...	...	0.938(2)	0.467(7)
0.5 $I_3 = 0$	...	...	0.917(3)	0.453(9)



Table III. The most successful fits were to data on  $48^3$  with  $\mu = 0.6$ , where straight line fits to data with  $k \leq \frac{3\pi}{8}$  proved possible. For  $\mu \leq 0.4$ , the fits only included data with  $k \leq \frac{\pi}{8}$  ( $48^3$ ) or  $k \leq \frac{3\pi}{16}$  ( $32^2 \times 48$ ). The general trend revealed in Table III is that the speed ratio  $s$  increases towards unity as  $\mu$  increases, and that the slope parameter  $F$  decreases slightly. Since the momentum resolution on  $32^2 \times 48$  is markedly worse, we can only comment on the absence of evidence for any significant finite volume effects, and, in the model with global  $SU(2) \otimes SU(2)$  symmetry, for any significant difference between isosinglet ( $\omega$ ) and isotriplet ( $\rho$ ) channels.

The most interesting comparison is between  $Z_2$  data on  $48^3$  with  $g^{-2} = 0.6$  and  $0.75$ , the stronger coupling corresponding to roughly a factor of 2 increase in lattice spacing; if we restore explicit factors of  $a$ , we see that the slope parameter  $Fa^{-1}$  remains roughly constant under this change, implying that the slope is a lattice artifact which should vanish in the continuum limit. At first sight, it is a little strange to observe an  $O(a)$  scaling violation in a simulation with staggered fermions. However, a careful analysis [14] reveals that there are indeed  $O(a)$  discretization artifacts in the lattice formulation of the GN interaction term  $(\bar{\psi}\psi)^2$ . This highlights that the effect we are examining is a property of an interacting system, since noninteracting staggered fermions show discretization effects only at  $O(a^2)$ . Since  $s$  also increases as the coupling is strengthened, we deduce a systematic effect as  $\mu a$  and hence  $\mu/T$  increase.

## V. DISCUSSION

We have, in Sec. III, used the Fermi liquid interaction to leading nontrivial order in  $1/N_f$  to find solutions to the Boltzmann equation corresponding to zero sound. The excitation is spin and isospin symmetric, and has speed  $s = \beta_0/\beta_F > 1$  for almost all  $\mu > \mu_c$ . In the simulations described in Sec. IV we have found a massless pole in a particular mesonic channel, interpolated by a staggered fermion bilinear point-split along the direction of propagation, with continuum quantum numbers corresponding to a local fluctuation in baryon density, with speed  $s \approx 1$ . To what extent can we be sure these results describe the same physical phenomenon?

Our solution based on the ansatz (12), is the unique one (symmetric in internal quantum numbers) which is a meromorphic function of  $z = e^{i\theta}$ . As remarked above, the poles fall on the real axis, yielding a real  $s > 1$ . Solutions with  $s < 1$  must therefore be of a different form to (12), and probably involve a branch cut ending inside the  $|z| = 1$  contour. We can see this physically by considering the emission of a phonon with momentum  $\vec{q}$  and energy  $\beta_0|\vec{q}|$  from a quasiparticle with momentum  $\vec{k}$  and energy  $\mu + \beta_F(|\vec{k}| - k_F)$ . This is allowed kinematically for  $s < 1$ , the angle of emission  $\phi$  satisfying

$$\cos\phi = s + \frac{|\vec{q}|}{2|\vec{k}|}(1 - s^2) > s. \quad (31)$$

All radiation is emitted within a cone of half-angle  $\cos^{-1}s$  centered on the quasiparticle trajectory. This well-known phenomenon is variously known as Landau damping, Čerenkov radiation, or most appropriately in the current context, as a sonic boom.

First let us argue how our numerical results can support a state resembling a simple pole but with  $s < 1$ , in apparent contradiction to the above. On a spacetime lattice, the radiation process is constrained because there is a natural lower bound for the angle of emission,  $\phi_{\min} \sim 2\pi/L_s|\vec{q}|$ . Landau damping is thus kinematically forbidden for

$$s > \cos\phi_{\min} \approx 1 - \frac{2\pi}{L_s^2|\vec{q}|^2}. \quad (32)$$

With a conservatively high  $|\vec{q}| \sim \mu/2$ , then on a  $48^3$  lattice we have no damping for  $s > 0.73$  at  $\mu = 0.2$ , rising to  $s > 0.97$  at  $\mu = 0.6$ . It is plausible therefore that damping is suppressed and that the phonon found in Sec. IV is described by an isolated pole even if  $s < 1$ .

Figure 6 suggests that  $s$  increases towards one as  $\mu$  increases. This contradicts the analytic solution shown in Fig. 1, which has  $\lim_{\mu \rightarrow \infty} s \rightarrow 1_+$ ; note, however, the disparity in vertical scale between the two figures. Simulations on volumes considerably larger than those used here will be needed to disentangle the various possible systematic effects due to finite  $L_s$ , finite  $\mu/T$ , and nonzero  $a$  in order to determine the sign of  $s - 1$  for finite  $N_f$ . We think the most probable explanation for  $s < 1$  is an effect of nonzero  $T \equiv (aL_t)^{-1}$ ; the physical temperature of the  $L_t = 48$  lattice decreases by a factor of roughly two going from  $g^{-2} = 0.75$  to  $g^{-2} = 0.6$ , and Table III has  $|s - 1|$  decreasing by roughly the same factor. While an extension of the analytic solution of Sec. III to  $T > 0$  is considerably beyond the scope of this work, it is known empirically that the speed of sound in liquid  $^3\text{He}$  *increases* as  $T \rightarrow 0$  and the dominant mode of propagation changes from first sound to zero sound [13].

An important element of our argument is that the phonon propagates at a speed  $\beta_0 \sim \beta_F^{\text{bare}} < 1$ , and is hence a Fermi surface phenomenon. In principle, since our extracted value of  $s \approx 1$  has relied on a rescaling of  $\beta_F$  to take account of discretization artifacts, we also need to go to considerably finer lattices, i.e., with  $\beta_F^{\text{bare}} \approx 1$ , in order to demonstrate a clear distinction between our signal and first sound with expected propagation speed  $\beta_1 \approx 0.7$ . If, however, the theoretical arguments about zero sound dominating as  $T \rightarrow 0$  can be taken seriously, then for the first time we have succeeded in identifying a collective oscillation in a lattice simulation.

## ACKNOWLEDGMENTS

S. J. H. was supported by a PPARC Senior Research Fellowship, and thanks the Institute for Nuclear Theory

at the University of Washington for its hospitality and the Department of Energy for partial support during the completion of this work.

- 
- [1] J. B. Kogut, D. K. Sinclair, S. J. Hands, and S. E. Morrison, Phys. Rev. D **64**, 094505 (2001).
  - [2] S. Muroya, A. Nakamura, and C. Nonaka, Phys. Lett. B **551**, 305 (2003).
  - [3] S. J. Hands and S. E. Morrison, Phys. Rev. D **59**, 116002 (1999).
  - [4] S. J. Hands, B. Lucini, and S. E. Morrison, Phys. Rev. D **65**, 036004 (2002).
  - [5] S. J. Hands and D. N. Walters, Phys. Rev. D **69**, 076011 (2004).
  - [6] S. J. Hands, J. B. Kogut, C. G. Strouthos, and T. N. Tran, Phys. Rev. D **68**, 016005 (2003).
  - [7] S. J. Hands, Nucl. Phys. A **642**, 228 (1998).
  - [8] L. D. Landau, Zh. Eksp. Teor. Fiz. **30**, 1058 (1956); Sov. Phys. JETP **3**, 920 (1956).
  - [9] L. D. Landau, Zh. Eksp. Teor. Fiz. **32**, 59 (1957); Sov. Phys. JETP **5**, 101 (1957).
  - [10] E. M. Lifshitz and L. P. Pitaevskii, *Statistical Physics (Part 2)* (Pergamon, Oxford, 1980), Vol. 9.
  - [11] L. D. Landau, Zh. Eksp. Teor. Fiz. **35**, 97 (1959); Sov. Phys. JETP **8**, 70 (1959).
  - [12] G. Baym and S. A. Chin, Nucl. Phys. A **262**, 527 (1976).
  - [13] A. A. Abrikosov, L. P. Gor'kov, and I. E. Dzyaloshinski, *Methods of Quantum Field Theory in Statistical Physics* (Dover, New York, 1963) Chap. 4; J. W. Negele and H. Orland, *Quantum Many-Particle Systems* (Westview Press, Boulder, 1988) Chap. 6.
  - [14] S. J. Hands, A. Kocić, and J. B. Kogut, Ann. Phys. (N.Y.) **224**, 29 (1993).
  - [15] C. Burden and A. N. Burkitt, Europhys. Lett. **3**, 545 (1987).